

Harnessing the Untapped Catalytic Potential of a $\text{CoFe}_2\text{O}_4/\text{Mn-BDC}$ Hybrid MOF Composite for Obtaining a Multitude of 1,4-Disubstituted 1,2,3-Triazole Scaffolds

Sneha Yadav, Shivani Sharma, Sriparna Dutta, Aditi Sharma, Alok Adholeya, and Rakesh K. Sharma*



Cite This: <https://dx.doi.org/10.1021/acs.inorgchem.0c00752>



Read Online

ACCESS |



Metrics & More

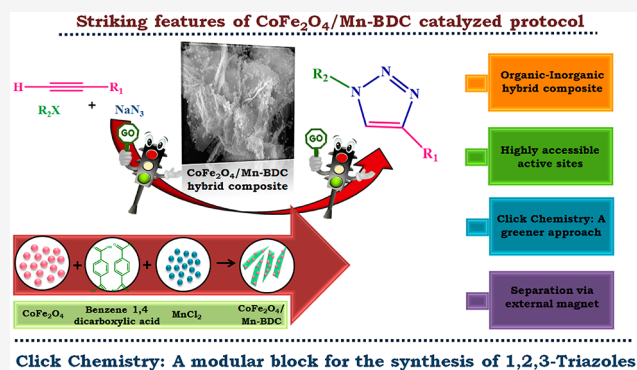


Article Recommendations



Supporting Information

ABSTRACT: Metal–organic frameworks derived nanostructures with extraordinary variability, and many unprecedented properties have recently emerged as promising catalytic materials to address the challenges in the field of modern organic synthesis. In this contribution, the present work reports the fabrication of an intricately designed magnetic MOF composite based on Mn-BDC (manganese benzene-1,4-dicarboxylate/manganese terephthalate) microflakes via a facile and benign in situ solvothermal approach. Structural information about the as-synthesized hybrid composite has been obtained with characterization techniques such as TEM, SEM, XRD, FT-IR, AAS, EDX, ED-XRF, and VSM analysis. Upon investigation of catalytic performance, the resulting material unveils remarkable efficacy toward facile access of a diverse array of pharmaceutically active 1,2,3-triazoles from a multicomponent coupling reaction of terminal alkynes, sodium azide, and alkyl or aryl halides as coupling partners. In addition to a wide substrate scope, the catalyst with highly accessible active sites also possesses a stable catalytic metal center along with superb magnetic properties that facilitate rapid and efficient separation. The prominent feature that makes this protocol highly desirable is the ambient and greener reaction conditions in comparison to literature precedents reported to date. Further, a plausible mechanistic pathway is also proposed to rationalize the impressive potential of the developed catalytic system in the concerned reaction. We envision that findings from our study would not only provide new insights into the judicious design of advanced MOF based architectures but also pave the way toward greening of industrial manufacturing processes to tackle critical environmental and economic issues.

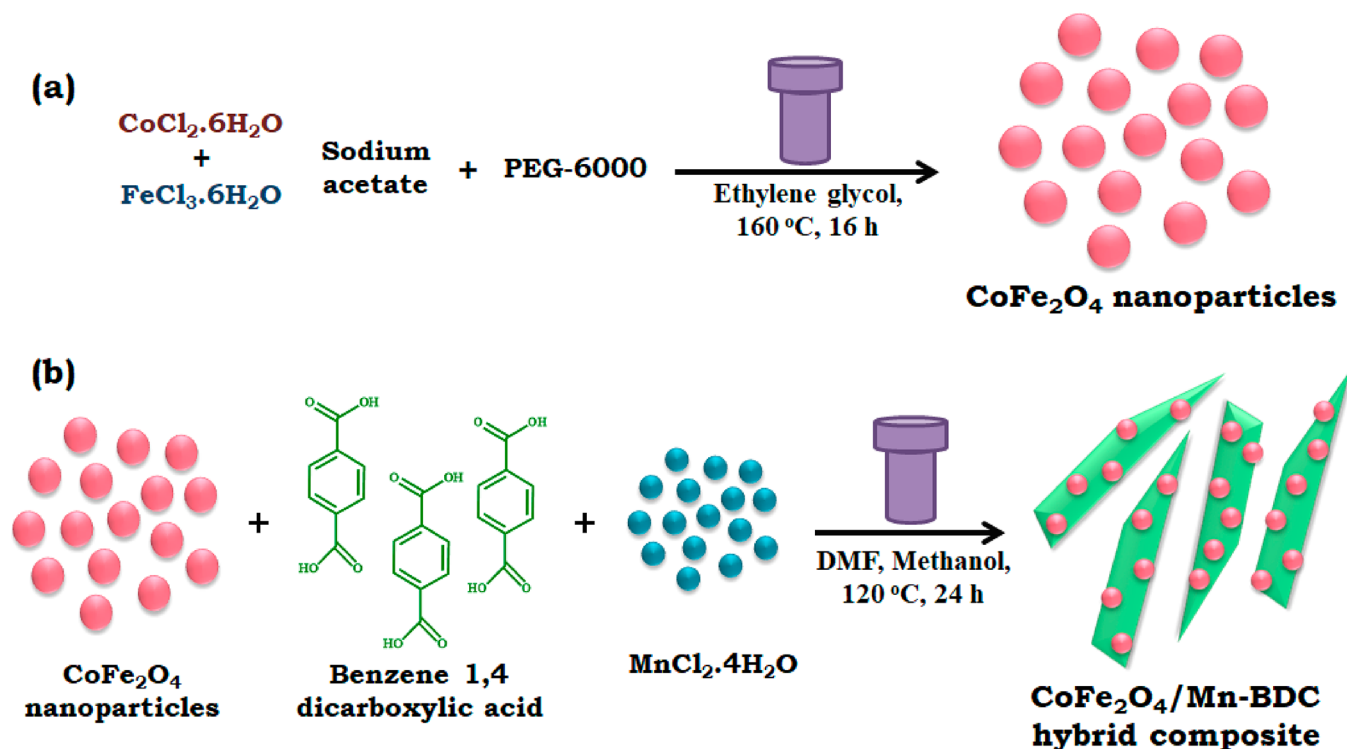


INTRODUCTION

The pioneering and seminal discovery of metal organic frameworks by a renowned chemist, Omar Yaghi, has sparked tremendous fascination among the scientific community worldwide. Ever since, research on the fundamental design and exploration of this intriguing class of materials continues to expand at an impressive pace.^{1–7} This upsurge of interest can be predominantly attributed to the possibility of modifying the organic as well as inorganic building blocks that provide invincible strategies to produce the controlled targeted MOFs.^{8–10} In addition, the phenomenal substructure of MOFs also endows them with several other marvelous attributes such as facile variability of the pore size, assorted topologies, unprecedented high surface area, and large pore volumes.^{11,12} Owing to the aforementioned remarkable aspects, these unique architectures greatly revolutionized the diverse emerging disciplines of catalysis, adsorption, gas storage, sensing, and separation.^{13–16} In particular, MOF based materials have marked a significant breakthrough in the arena of heterogeneous catalysis since their crystal chemistry

prevents deactivation of the catalytic system as a result of the well separated arrangement of metal clusters by organic ligands that accentuate their enduring efficiency.^{17–25} Indeed, integration of MOFs' functional properties with the magnetic properties of nanoparticles to obtain hybrid materials has aroused broad interest, as it not only dramatically enhances catalytic performance and durability but also facilitates expedient separation under the influence of external magnetic forces.^{26–31} Driven by such innovations, tremendous endeavors are directed toward the quest of novel catalysts to improve previously unexplored organic transformations. In this context, a comprehensive literature survey reveals the scope of advancement in click chemistry that has been creating a

Received: March 12, 2020

Scheme 1. Synthesis of $\text{CoFe}_2\text{O}_4/\text{Mn-BDC}$ Hybrid Composite

renaissance in modern synthetic chemistry for the construction of ubiquitous carbon–heteroatom bonds.^{32–35} Among various modular click approaches, Huisgen cycloaddition involving terminal alkynes and azides as substrates is the well-known synthetic route to furnish 1,2,3-triazoles with magnificent biological and therapeutic activities.^{36–39} Even a few triazole derivatives, for example, cefatrizine, *tert*-butyldimethylsilylspiraminoxathioledioxide, and Tazobactam, possess anticancer, antiviral, and antibiotic properties.^{40–43} However, the premier cycloaddition route encountered serious drawbacks of difficult isolation and handling of toxic organic azides, which have prompted chemists and engineers to design other synthetic reaction pathways. Consequently, an alternative one pot strategy has been explored wherein in situ organic azide facilitates the access of entwined structures via click coupling among terminal alkynes, sodium azide, and alkyl/aryl halides.^{44–52} Despite intensive efforts, none of the aforementioned methodologies have the potential to entirely address the formidable challenges often encountered in practical implications in pharmaceutical and medicinal industries. Severe limitations associated with these reported metal catalyzed transformations include harsh reaction conditions, a high temperature, low product yield, the use of additives, metal contamination, toxic solvents, catalyst reusability, leaching of active species, and many more. Therefore, the current status reveals the imperative need to explore new catalytic materials which can not only effectively deal with the aforesaid issues but also simultaneously meet the criteria of sustainability.

In our persistent research interests in exploring benign strategies for obtaining organic–inorganic composites and their exploitation as potent adsorbents and catalytic systems,^{53–59} we hereby elucidate the fabrication of a hybrid $\text{CoFe}_2\text{O}_4/\text{Mn-BDC}$ MOF composite endowed with superparamagnetic properties through a facile in situ solvothermal approach. The developed intricately designed material unveils

magnificent catalytic performance in one-pot “click” coupling of terminal alkynes, aryl or alkyl halides, and sodium azide to obtain diverse triazole motifs with extraordinary pharmacological activities that can easily be metamorphosed into highly demanding drugs. Some of the striking aspects that render this expeditious synthetic protocol a potentially benign and sustainable option over already existing routes are ambient reaction conditions, a high turnover number, economic viability, an operationally simple procedure, an environmentally benign solvent, ease in scaleup, excellent yields, short reaction times, no use of additives, excellent durability, and effortless magnetic recovery of the catalyst. To the best of our insight, this is the first attempt to evaluate the catalytic efficacy of three-dimensional magnetic Mn-BDC MOF material in the concerned one-pot “click” reaction. In view of these considerations, we foresee that the current research work would not only enlighten the scientific community about the rational design of advanced MOF based architectures but also outline new directions in medicinal fields to access novel generic drugs in an eco-friendly manner.

EXPERIMENTAL SECTION

Materials and Reagents. Benzene 1,4 dicarboxylic acid (1,4-BDC) was procured from Tokyo Chemical Industry (TCI) Pvt. Ltd. Ferric chloride hexahydrate, cobalt chloride hexahydrate, and manganese chloride tetrahydrate were all obtained from Sisco Research Laboratories (SRL) Pvt. Ltd. The rest of the reagents and starting precursors were purchased from Spectrochem Private Limited.

Instrumentation. A PerkinElmer Spectrum 2000 was used to record Fourier transform infrared (FT-IR) plots of all the developed materials in the range of 4000–400 cm^{-1} using KBr. The size and shape of developed composites were determined through transmission electron microscopy (TEM) micrographs obtained from FEI TECHNAI G² T20 at 200 kV. In addition, scanning electron microscopy (SEM) images of synthesized materials were captured

through a Jeol scanning electron microscope. Both compositional analysis as well as elemental mapping of fabricated composites was acquired from EDX equipment fitted with a SEM instrument. A Bruker D8 Advance instrument was employed to obtain powder X-ray diffraction data of designed materials in the 2θ range of $5\text{--}80^\circ$ working at a scanning rate of 3° min^{-1} . For dispersion, developed nanoparticles were sonicated using a Tekmar Sonic Disruptor (model TM300). Flame atomic absorption spectroscopy was employed to calculate loading of the manganese in the final catalyst using N3180021 PinAAcle 500. Prepared nanoparticles and hybrid composites were subjected to vibrating sample magnetometry analysis wherein the magnetic field was varied from -10000 to 10000 Oe at room temperature (r.t.) via EV-9, Microsense, ADE. Successful synthesis of triazoles was affirmed using GC-MS analysis on an Agilent gas chromatogram (6850 GC) with a HP-5MS 5% phenylmethyl siloxane capillary column ($30.0 \text{ m} \times 250 \mu\text{m} \times 0.25 \mu\text{m}$) and a quadrupole mass filter equipped with a 5975 mass selective detector (MSD) using helium as the carrier gas. A JEOL JNM-EXCP-400 instrument was used to record ^1H and ^{13}C NMR of obtained triazole derivatives.

Synthesis of Catalyst. Preparation of CoFe_2O_4 . The developed magnetic MOF composite was synthesized in a stepwise manner, out of which the first step included the synthesis of CoFe_2O_4 using a solvothermal synthetic strategy.⁶⁰ In a typical procedure, 148.7 mg of $\text{CoCl}_2 \cdot 6\text{H}_2\text{O}$ and 337.9 mg of $\text{FeCl}_3 \cdot 6\text{H}_2\text{O}$ were dissolved homogeneously in 10 mL of ethylene glycol at 50°C under magnetic stirring. Thereafter, sodium acetate (900 mg) and PEG-6000 (500 mg) were sequentially mixed into the above solution while stirring. After being continuously stirred for 30 min , the as obtained homogeneous mixture was subsequently transferred to an autoclave maintained at 160°C for 16 h . The resulting black colored CoFe_2O_4 precipitate was isolated via an external magnet, which was further washed several times using double-deionized water and eventually dried at 60°C for 6 h .

Preparation of Manganese Terephthalic Acid Metal Organic Framework (Mn-BDC). Mn-BDC was synthesized using a procedure reported by Shen and co-workers.⁶¹ First of all, $\text{MnCl}_2 \cdot 4\text{H}_2\text{O}$ (0.76 g) and 1,4-BDC (0.83 g) were added to a round-bottom (R.B.) flask containing 40 mL of DMF and kept under magnetic stirring. This step was followed by the addition of 10 mL of methanol, and the resulting solution was kept under stirring for a further 10 min to obtain a homogeneous solution. The solution so obtained was transferred to an autoclave held at 120°C for 24 h . The so formed solid powder was filtered, washed using methanol, and finally dried at 110°C for 24 h in an oven.

Preparation of MOFs Decorated CoFe_2O_4 Nanoparticles ($\text{CoFe}_2\text{O}_4/\text{Mn-BDC}$). The $\text{CoFe}_2\text{O}_4/\text{Mn-BDC}$ hybrid composite was synthesized using a facile procedure (Scheme 1). For this, $\text{MnCl}_2 \cdot 4\text{H}_2\text{O}$ (0.76 g) and 1,4-BDC (0.83 g) were added into an R.B. flask containing 40 mL of DMF under magnetic stirring to form a homogeneous solution. After this, 10 mL of methanol was added, and the resulting solution was stirred for another 10 min to obtain a homogeneous solution. After that, synthesized CoFe_2O_4 nanoparticles (0.4 g) were introduced into the above solution, and the overall assembly was then subjected to ultrasonication for 30 min . Eventually, the obtained solution was transferred to an autoclave and held at 120°C for 24 h . Finally, the obtained composite was magnetically separated, washed using methanol, and dried at 110°C for 24 h in an oven.

Procedure for $\text{CoFe}_2\text{O}_4/\text{Mn-BDC}$ Mediated Synthesis of 1,4-Disubstituted 1,2,3-Triazoles. Terminal alkyne (1 mmol), sodium azide (1 mmol), aryl or alkyl halide (1 mmol), and $\text{CoFe}_2\text{O}_4/\text{Mn-BDC}$ (25 mg) were added to an R.B. flask containing water (2 mL) and stirred at 50°C for the appropriate time period. The reaction was simultaneously monitored via TLC, and once the reaction was completed, the obtained reaction mixture was allowed to cool to room temperature. Thereafter, the catalyst was magnetically separated followed by extraction of the reaction mixture with ethyl acetate and water; the so formed organic layer was dried using anhydrous sodium

sulfate. Finally, GC-MS analysis of triazole products was carried out to authenticate their successful synthesis.

RESULTS AND DISCUSSION

The final catalyst was prepared as per Scheme 1. The first step involved in the fabrication of the overall composite is the synthesis of CoFe_2O_4 through a solvothermal preparation route. After that, the synthesized CoFe_2O_4 nanoparticles were added into the precursor salts of MOF to yield the $\text{CoFe}_2\text{O}_4/\text{Mn-BDC}$ hybrid composite. The final catalyst was then subjected to a series of characterization techniques including SEM, FT-IR, TEM, EDX, ED-XRF, XRD, VSM, and AAS.

Catalyst Characterizations. In order to affirm the presence of a functional group in the fabricated materials, these samples were subjected to FT-IR analysis, and data were recorded in the range of $4000\text{--}400 \text{ cm}^{-1}$. Figure 1 represents

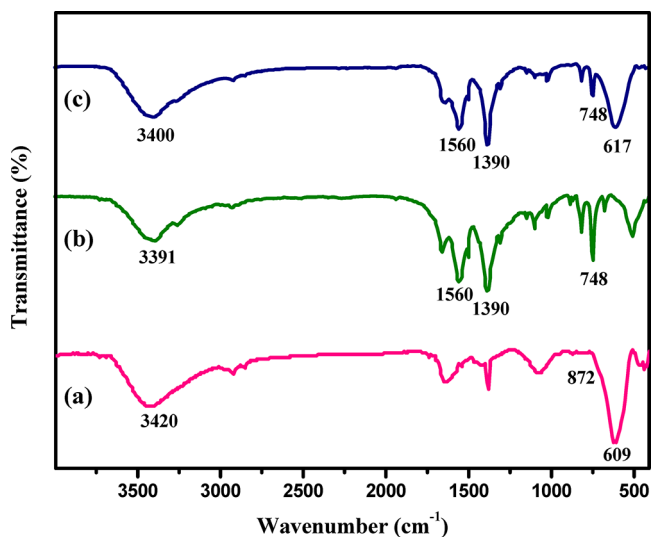


Figure 1. FTIR spectral plot of (a) CoFe_2O_4 , (b) Mn-BDC, and (c) $\text{CoFe}_2\text{O}_4/\text{Mn-BDC}$.

FTIR spectra of CoFe_2O_4 , Mn-BDC, and $\text{CoFe}_2\text{O}_4/\text{Mn-BDC}$. The CoFe_2O_4 spectrum reveals the presence of typical Fe–O and Co–O vibrations centered at around 609 and 872 cm^{-1} . In addition, the existence of surface hydroxyl (OH) groups on CoFe_2O_4 is confirmed by the presence of a broad band at around 3420 cm^{-1} .^{60,62} Further, in the FTIR spectrum of Mn-BDC, the appearance of two peaks at 1390 and 1560 cm^{-1} corresponds to stretching vibrations (symmetric and asymmetric, respectively) in the organic ligands due to COO^- groups. In addition to this, the existence of a peak at 748 cm^{-1} clearly illustrates the effective coordination of manganese ions to 1,4-BDC. Furthermore, a comparison of the FTIR spectra of cobalt ferrite and the final catalyst successfully confirms the decoration of Mn-BDC MOF with inverse spinel CoFe_2O_4 . The final catalyst spectra exhibit that bands at 1560 , 1390 , and 748 cm^{-1} are ascribed to the MOF, while the band around 617 cm^{-1} is due to the Fe–O vibrations of the CoFe_2O_4 .

Knowledge of the structural integrity and crystallinity of developed hybrid composites was gained through XRD analysis (Figure 2) of CoFe_2O_4 , Mn-BDC, and $\text{CoFe}_2\text{O}_4/\text{Mn-BDC}$. The CoFe_2O_4 XRD pattern reveals the presence of diffraction peaks at $2\theta = 30.4^\circ$, 35.7° , 43.4° , 53.7° , 57.2° , and 62.7° which correspond to the (220), (311), (400), (422), (511), and (440) planes. The observed 2θ diffraction values

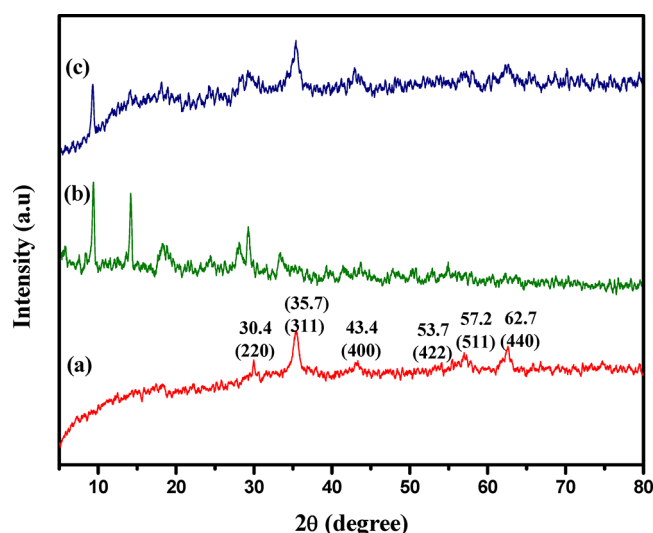


Figure 2. XRD spectral plot of (a) CoFe_2O_4 , (b) Mn-BDC, and (c) $\text{CoFe}_2\text{O}_4/\text{Mn-BDC}$.

are in good agreement with the CoFe_2O_4 data in JCPDS (card number: 22-1086; Figure S1).⁶⁰ Additionally, in the XRD spectra of Mn-BDC, diffraction peaks at 9.4° , 14.2° , 18.8° , 19.3° , 24.4° , 28.2° , 29.4° , and 33.6° match with a simulated XRD plot generated utilizing previously reported single crystal X-ray data⁶³ and thus confirm the successful synthesis of the Mn-BDC framework (Figure S2). It is also evident from the PXRD spectra of Mn-BDC that it possesses a crystalline structure. Finally, the emerging peaks from the XRD spectrum of the $\text{CoFe}_2\text{O}_4/\text{Mn-BDC}$ composite belong to both CoFe_2O_4 and Mn-BDC, suggesting the successful decoration of CoFe_2O_4 nanoparticles onto the Mn-BDC.

TEM and SEM are considered to be one of the highly powerful techniques that throw light not only on morphological features but also on the size of designed composites. TEM and SEM images of these hybrid materials have been provided in Figure 3. A TEM image of CoFe_2O_4 (Figure 3d) divulges the formation of spherical shaped nanoparticles having a diameter of approximately 200 nm. CoFe_2O_4 SEM analysis (Figure 3a) also discloses the fabrication of monodisperse nanoparticles with a spherical morphology. In addition, SEM and TEM images of bare Mn-BDC (Figure 3b and e) clearly show that the synthesized MOF has a homogeneous laminar microflake-like structure. Moreover, the SEM image of $\text{CoFe}_2\text{O}_4/\text{Mn-BDC}$ (Figure 3c) shows the presence of dispersed magnetic inverse spinel cobalt ferrite nanoparticles on the surface of bare Mn-BDC, which further validates the successful preparation of the hybrid heterostructures.

EDX with elemental mapping was employed for the compositional analysis of the synthesized composites. Elemental mapping images of the hybrid $\text{CoFe}_2\text{O}_4/\text{Mn-BDC}$ material reveals that it is composed of five elements, namely, Co, Fe, O, Mn, and C (Figure 4). On the basis of results obtained from elemental analysis, the loading of CoFe_2O_4 nanoparticles in the hybrid composite was found to be approximately 36% (Table S1). In addition, the EDX spectrum of CoFe_2O_4 shows distinct peaks of Co, Fe, and O, while the EDX spectrum of $\text{CoFe}_2\text{O}_4/\text{Mn-BDC}$ indicates the appearance of well-defined peaks of Mn and C in addition to Co, Fe, and O, which further provides a concrete proof of the overall synthetic process (Figure 5). Moreover, ED-XRF of $\text{CoFe}_2\text{O}_4/\text{Mn-BDC}$ also shows peaks of Mn, Co, and Fe further providing a vital clue for the synthesis of a hybrid heterostructure. In addition, quantitative estimation of the final hybrid catalytic system was carried out using the AAS

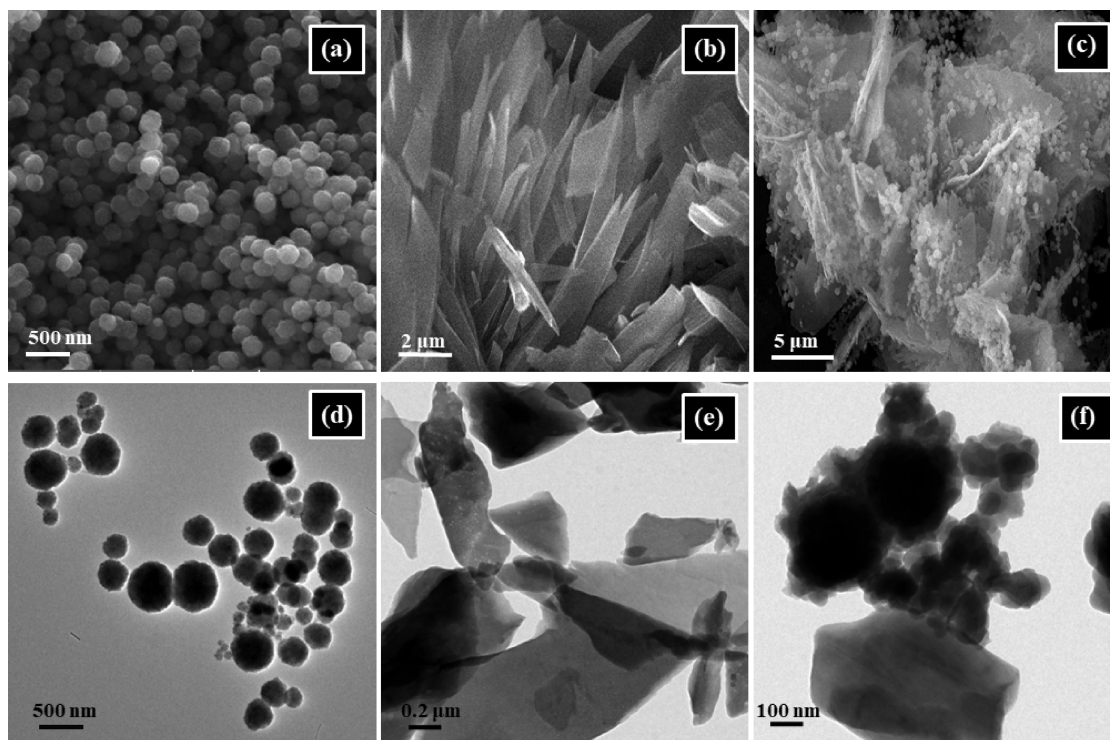


Figure 3. SEM micrographs of (a) CoFe_2O_4 , (b) Mn-BDC, and (c) $\text{CoFe}_2\text{O}_4/\text{Mn-BDC}$ and TEM micrographs of (d) CoFe_2O_4 , (e) Mn-BDC, and (f) $\text{CoFe}_2\text{O}_4/\text{Mn-BDC}$.

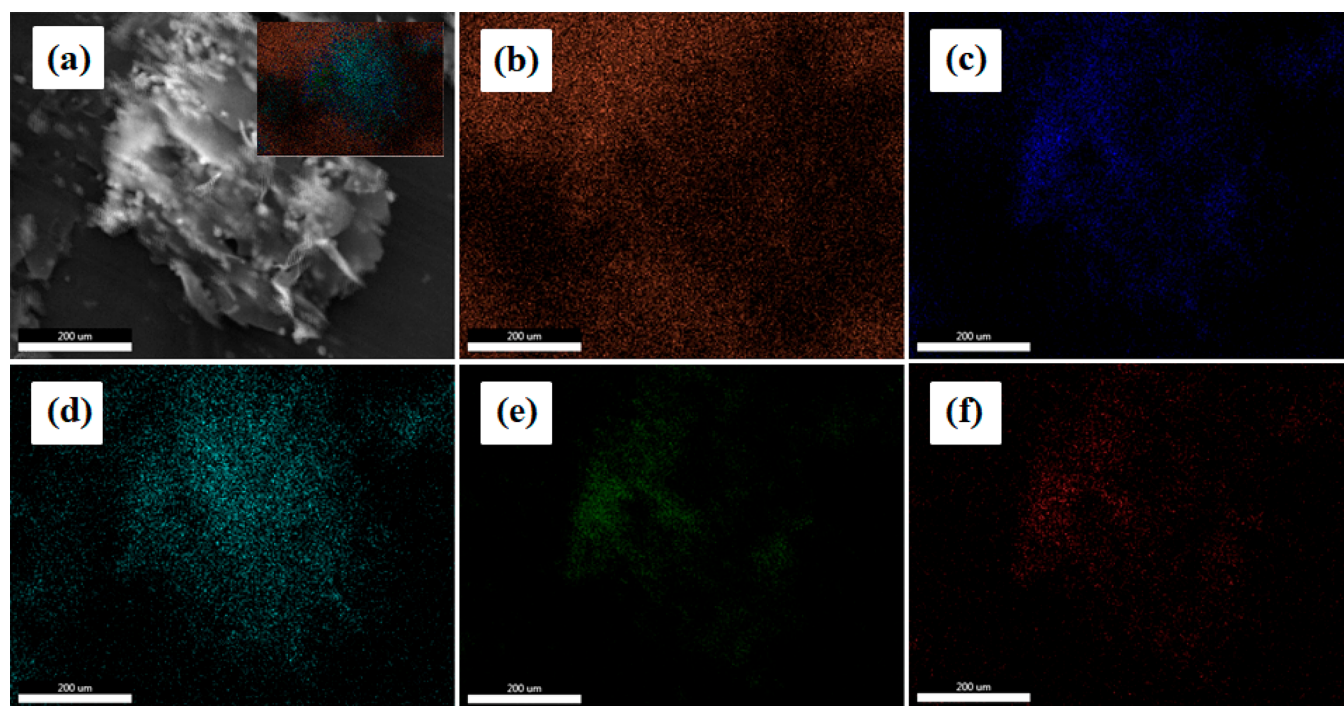


Figure 4. (a) SEM of CoFe₂O₄/Mn-BDC hybrid composite and the corresponding elemental mapping analysis of (b) C, (c) O, (d) Mn, (e) Fe, and (f) Co in the catalyst.

technique, which reveals that 0.499 mmol/g of manganese is present in CoFe₂O₄/Mn-BDC.

VSM analysis was employed to study magnetic properties of CoFe₂O₄, Mn-BDC, and CoFe₂O₄/Mn-BDC under a magnetic field varied from $-10,000$ to $10,000$ Oe at r.t. (Figure 6). Further, superparamagnetic behavior of synthesized composites is confirmed by the magnetic hysteresis curves, exhibiting no obvious remanence and coercivity. In addition, it is found that the CoFe₂O₄ saturation magnetization (M_s) value is 57 emu/g, while Mn-BDC does not possess any magnetic character. However, upon integration with nonmagnetic Mn-BDC, a decrease in CoFe₂O₄ saturation magnetization is observed from 57 to 22 emu/g. Nevertheless, the saturation magnetization value of CoFe₂O₄/Mn-BDC is sufficient enough as it allows its complete, efficient, and rapid removal via an external magnetic force.

Activity of CoFe₂O₄/Mn-BDC in Click Coupling Reaction to Afford 1,4-Disubstituted 1,2,3-Triazoles. Catalytic competence of the newly fabricated CoFe₂O₄/Mn-BDC hybrid composite was explored in the multicomponent click protocol to access 1,4-disubstituted 1,2,3-triazoles. In addition, the effects of several thermodynamic and kinetic parameters including time, solvent, temperature, and amount of catalyst were studied for multicomponent click coupling.

In our preliminary reactivity tests, phenylacetylene and benzyl bromide were chosen as model substrates, and the results are compiled in Table 1. Initially the model reaction was performed in water at 50 °C for 2 h without a catalyst. However, the reaction failed to occur, further necessitating the need of a catalyst (entry 1, Table 1). After the addition of CoFe₂O₄/Mn-BDC into the same reaction system, 100% conversion percentage was detected after 2 h (entry 2). Additionally, CoFe₂O₄ nanoparticles also catalyzed the reaction with lower conversion percentage (entry 3). We further examined other solvents under the same conditions

using CoFe₂O₄/Mn-BDC as the catalyst, but the results were not satisfactory (entries 4–6). The solvent screening studies indicate that water behaves as the best solvent for this reaction. Furthermore, reaction was carried out for discrete time periods, yet the results were very inferior (entries 7 and 8). Next, the variation in amount of catalyst in the concerned reaction was investigated (entry 9). As evident through GC-MS, conversion percentage was found to decrease on decreasing the amount of catalyst. Further assessment of the temperature conditions were carried out (entries 10 and 11). Both an increase and decrease in temperature resulted in lower conversion percentage. A variety of metal salts were further screened for their ability to stimulate the multicomponent click reaction. Adversely, the metal salts were totally ineffective in promoting the reaction (entries 12 and 13). Apart from this, the test reaction was also carried out with bare Mn-BDC, which also results in good conversion percentage (entry 14). Thus, the optimal reaction conditions were considered to include phenylacetylene (1 mmol), sodium azide (1 mmol), benzyl bromide (1 mmol), CoFe₂O₄/Mn-BDC (25 mg), and water as the solvent at 50 °C for 2 h.

Substrate Scope. In a quest to broaden the versatility of the designed hybrid composite, its catalytic efficiency has been assessed for a wide array of substituted phenylacetylenes and aryl halides under the optimized parameters (Table 2). Several features of this simple and inexpensive protocol are worth applauding. To our delight, when various terminal alkynes were subjected to the reaction under optimized conditions, triazole products were obtained with excellent conversion percentage. Next, the scope of a series of aryl halides was explored in the concerned reaction. The results revealed that the reaction also proceeded well with substituted benzyl chloride and benzyl bromide. The unsubstituted phenylacetylene gave 100% conversion percentage, while with the substituted phenylacetylenes, the conversion percentage

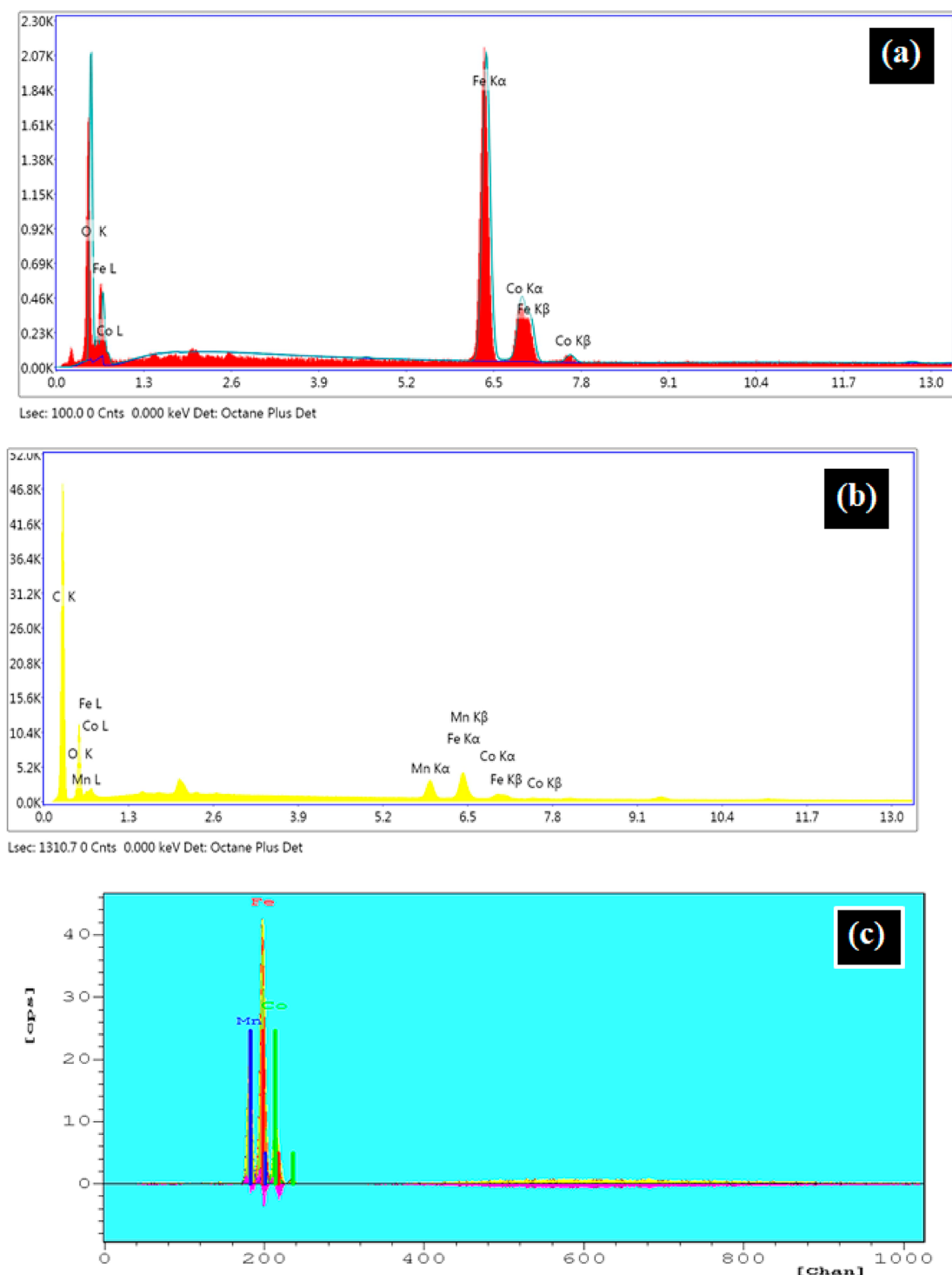


Figure 5. EDX of (a) CoFe₂O₄, (b) CoFe₂O₄/Mn-BDC, and (c) EDXRF of CoFe₂O₄/Mn-BDC hybrid composite.

decreased with the increasing electron donating capability of the substituents. This is evident from Table 2, entries 3, 8, and 10, which show that the conversion percentage is 96%, 24%, and 9% for 4-*tert* butyl phenylacetylene, 4-methyl phenylacetylene, and 4-methoxy phenylacetylene, respectively. Furthermore, the protocol was extended to aliphatic halides such as *n*-butyl bromide, which gave satisfactory results. Notably, the present click reaction not only exhibits wide substrate scope and high conversion percentage but also solely ends up in the formation of 1,4-disubstituted 1,2,3-triazoles.

Mechanistic Pathway. Scheme 2 illustrates a plausible mechanistic pathway for the concerned reaction using CoFe₂O₄/Mn-BDC as the catalyst. Initially, coordination between the magnetic Mn-BDC MOF based catalyst and the terminal alkyne forms a manganese coordinated acetylene complex (A), which is a better dienophile than acetylene itself. Simultaneously, alkyl halide upon in situ reaction with sodium azide results in the generation of an alkyl azide intermediate, which subsequently interacts with complex A to form complex B. This complex (B) further undergoes a 1,3-dipolar

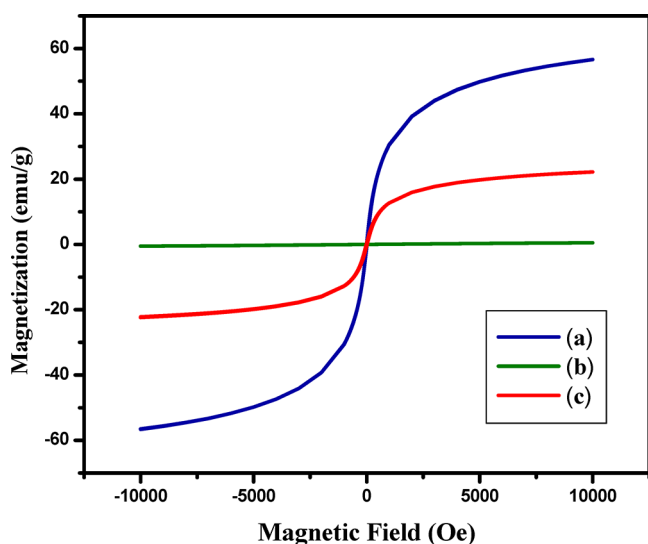


Figure 6. VSM of (a) CoFe_2O_4 , (b) Mn-BDC, and (c) $\text{CoFe}_2\text{O}_4/\text{Mn-BDC}$ hybrid composite.

cycloaddition reaction to generate complex C. Finally, complex C affords the desired 1,2,3-triazole moieties (D) with the regeneration of $\text{CoFe}_2\text{O}_4/\text{Mn-BDC}$.

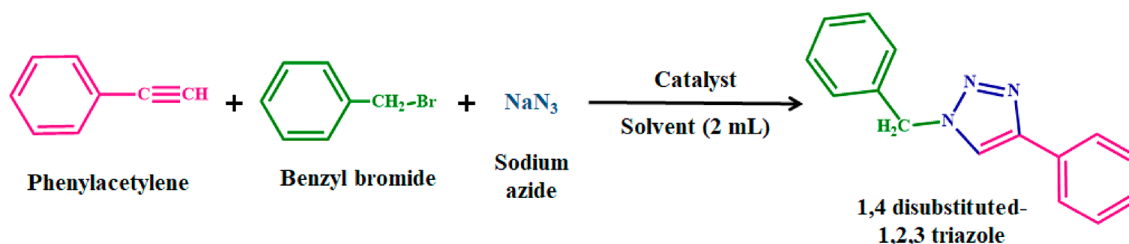
Heterogeneity and Recyclability Tests. With the aim of determining the intrinsic stability of the designed $\text{CoFe}_2\text{O}_4/\text{Mn-BDC}$ hybrid catalyst, a standard heterogeneity test was conducted in which the test substrates (phenylacetylene and benzyl bromide) were again subjected to optimized reaction conditions. Thereafter, $\text{CoFe}_2\text{O}_4/\text{Mn-BDC}$ was magnetically removed (after half the reaction time), while the reaction was further allowed to proceed for a prolonged duration. The absence of a leached catalytic metal center in the supernatant

was confirmed through GC-MS. Once the $\text{CoFe}_2\text{O}_4/\text{Mn-BDC}$ was taken out from the reaction media, there was no further increment in conversion percentage, which clearly debarred the probability of leached manganese metal from $\text{CoFe}_2\text{O}_4/\text{Mn-BDC}$.

Reusability and recyclability are the two most desired and indispensable parameters from an industrial and commercial perspective. Therefore, recyclability of the developed $\text{CoFe}_2\text{O}_4/\text{Mn-BDC}$ hybrid catalyst was tested in the concerned reaction using phenylacetylene and benzyl bromide as representative substrates. Thereafter, $\text{CoFe}_2\text{O}_4/\text{Mn-BDC}$ was retrieved under the influence of external magnetic forces upon the completion of the reaction, which was further washed with acetone and dried in an oven. Subsequently, the recovered $\text{CoFe}_2\text{O}_4/\text{Mn-BDC}$ was utilized again in the same reaction as shown in Figure 7, which clearly signifies the retainment of its catalytic efficacy up to five consecutive runs. Further, the high stability of the designed hybrid catalytic system is evident from SEM, VSM, and XRD (Figures S3, S4, and S5, respectively) of recovered $\text{CoFe}_2\text{O}_4/\text{Mn-BDC}$, which reveals that its morphology, magnetization, and crystallinity remained unchanged after catalysis.

Comparison of $\text{CoFe}_2\text{O}_4/\text{Mn-BDC}$ Activity with Reported Catalytic Materials. A critical comparison of the $\text{CoFe}_2\text{O}_4/\text{Mn-BDC}$ catalyzed protocol was made with those already reported in the literature, and the results are presented in Table S2. A thorough analysis of reports related to the concerned reaction concludes that this is first ever MOF composite catalyzed synthetic route to afford 1,4-disubstituted 1,2,3-triazoles. Indeed, it is splendid to say that the developed catalyst displayed its supremacy over the literature precedents when compared on the basis of substrate scope, turnover number, catalyst retrievability, and optimized parameters like time, temperature, etc. In addition, $\text{CoFe}_2\text{O}_4/\text{Mn-BDC}$

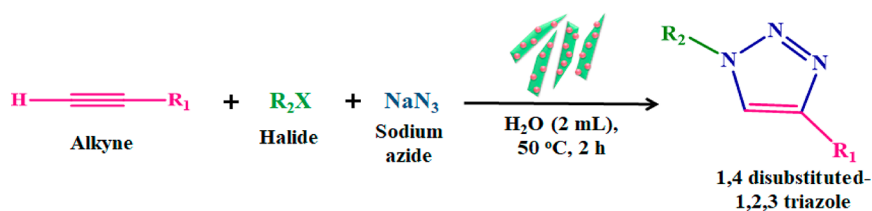
Table 1. Optimization of the Reaction Parameters^a



entry	catalyst	amount of catalyst (mg)	solvent (mL)	temp. (°C)	time (h)	conversion ^b (%)
1	no catalyst		water	50	2	
2	$\text{CoFe}_2\text{O}_4/\text{Mn-BDC}$	25	water	50	2	100
3	CoFe_2O_4	25	water	50	2	9
4	$\text{CoFe}_2\text{O}_4/\text{Mn-BDC}$	25	t-butanol	50	2	88
5	$\text{CoFe}_2\text{O}_4/\text{Mn-BDC}$	25	ethanol	50	2	20
6	$\text{CoFe}_2\text{O}_4/\text{Mn-BDC}$	25	acetonitrile	50	2	44
7	$\text{CoFe}_2\text{O}_4/\text{Mn-BDC}$	25	water	50	1	50
8	$\text{CoFe}_2\text{O}_4/\text{Mn-BDC}$	25	water	50	0.5	18
9	$\text{CoFe}_2\text{O}_4/\text{Mn-BDC}$	15	water	50	2	37
10	$\text{CoFe}_2\text{O}_4/\text{Mn-BDC}$	25	water	30	2	45
11	$\text{CoFe}_2\text{O}_4/\text{Mn-BDC}$	25	water	60	2	82
12	$\text{CoCl}_2 \cdot 6\text{H}_2\text{O}$	25	water	50	2	5
13	$\text{FeCl}_3 \cdot 6\text{H}_2\text{O}$	25	water	50	2	16
14	Mn-BDC	25	water	50	2	100

^aReaction conditions: Phenylacetylene (1 mmol), sodium azide (1 mmol), benzyl bromide (1 mmol), catalyst (x mg) and solvent (2 mL).

^bConversion percentages were determined via GC-MS.

Table 2. Synthesis of 1,4-Disubstituted 1,2,3-Triazoles Using CoFe₂O₄/Mn-BDC^a

Entry	Alkyne	Halide	Time (h)	Conversion ^b (%)	TON ^c
1.			2	100	801
2.			2	88	705
3.			2	96	793
4.			2	71	761
5.			2	25	200
6.			2	100	801
7.			2.5	68	545
8.			2	24	192
9.			2.5	31	248
10.			3	9	72

^aReaction conditions: Terminal alkyne (1 mmol), sodium azide (1 mmol), aryl/alkyl halide (1 mmol), CoFe₂O₄/Mn-BDC (25 mg), water (2 mL), 50 °C. ^bConversion percentages were obtained from GC-MS. ^cTON represents no. of moles of obtained product per mole of catalyst.

retained its integral structure as well as catalytic potential even after five subsequent catalytic runs.

CONCLUSION

In conclusion, a magnetically retrievable Mn-BDC hybrid MOF catalyst has been fabricated using a solvothermal synthetic route and subsequently characterized with a multitude of advanced physicochemical tools including TEM, SEM, VSM, FTIR, XRD, EDX, ED-XRF, and AAS. Thereafter,

catalytic performance of CoFe₂O₄/Mn-BDC is explored in click coupling to afford 1,4-disubstituted 1,2,3-triazoles. The adopted methodology being simple and operationally facile furnished several biologically and pharmaceutically significant molecules containing a triazole framework with satisfactory yield. On the basis of previous references pertaining to the concerned reaction, a tentative mechanism illustrating the role of the MOF based catalyst has been proposed. Furthermore, wider functional group tolerance, facile conditions, good

Scheme 2. Illustration of Plausible Mechanistic Route for the $\text{CoFe}_2\text{O}_4/\text{Mn-BDC}$ Mediated Synthesis of 1,4 Disubstituted 1,2,3-Triazoles

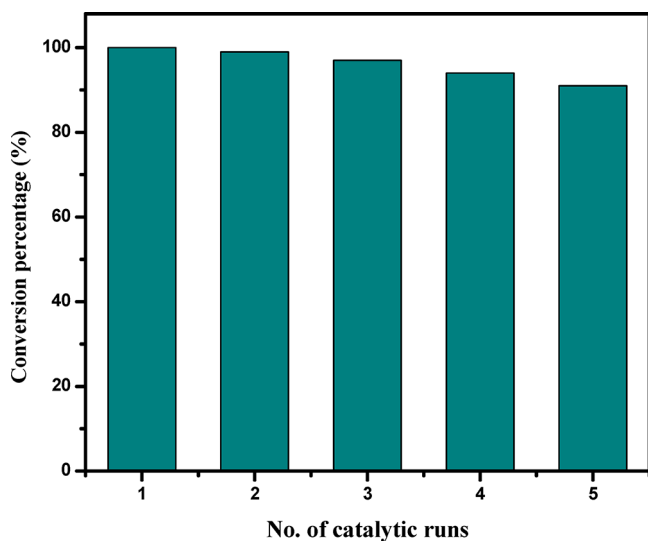
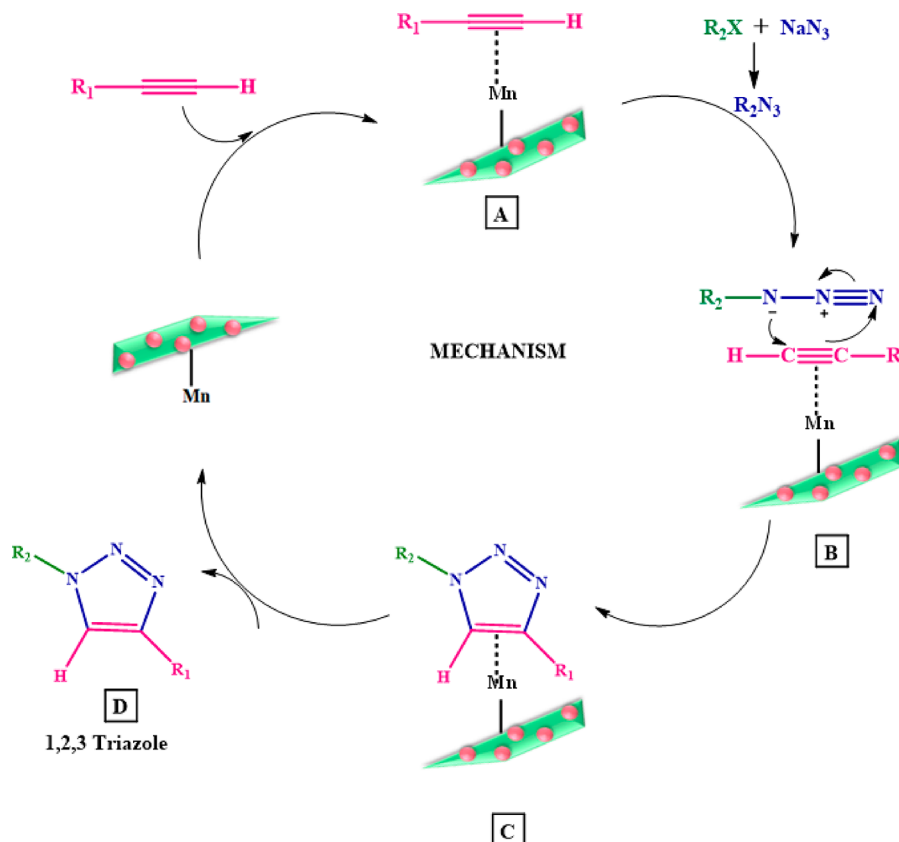


Figure 7. Recycling studies for the concerned reaction [reaction conditions: phenylacetylene (1 mmol), sodium azide (1 mmol), benzyl bromide (1 mmol), $\text{CoFe}_2\text{O}_4/\text{Mn-BDC}$ (25 mg), water (2 mL), 50 °C, 2 h].

turnover number, and atom economy are some of the intriguing features of this protocol that make it economically compatible and competitive in comparison to those already reported in the literature. In addition, $\text{CoFe}_2\text{O}_4/\text{Mn-BDC}$ in addition to facile retrievability through external magnetic forces can also be effectively reutilized for five subsequent catalytic runs.

■ ASSOCIATED CONTENT

Supporting Information

The Supporting Information is available free of charge at <https://pubs.acs.org/doi/10.1021/acs.inorgchem.0c00752>.

Comparison of CoFe_2O_4 PXRD with the database in JCPDS, Mn-BDC simulated XRD, characterizations (SEM, VSM, and XRD) of the recovered $\text{CoFe}_2\text{O}_4/\text{Mn-BDC}$, elemental mapping data of $\text{CoFe}_2\text{O}_4/\text{Mn-BDC}$, comparison of $\text{CoFe}_2\text{O}_4/\text{Mn-BDC}$ catalytic activity, GC-MS spectra of the synthesized products, ^1H and ^{13}C NMR of obtained triazoles (PDF)

■ AUTHOR INFORMATION

Corresponding Author

Rakesh K. Sharma — Green Chemistry Network Centre, Department of Chemistry, University of Delhi, New Delhi 110007, India; orcid.org/0000-0003-4281-876X; Phone: 011-276666250; Email: rkssharmagreenchem@hotmail.com; Fax: +91-011-27666250

Authors

Sneha Yadav — Green Chemistry Network Centre, Department of Chemistry, University of Delhi, New Delhi 110007, India

Shivani Sharma — Green Chemistry Network Centre, Department of Chemistry, University of Delhi, New Delhi 110007, India

Sriparna Dutta — Green Chemistry Network Centre, Department of Chemistry, University of Delhi, New Delhi 110007, India

Aditi Sharma — Green Chemistry Network Centre, Department of Chemistry, University of Delhi, New Delhi 110007, India

Alok Adholeya – TERI-Deakin Nanobiotechnology Centre,
TERI Gram, The Energy and Resources Institute, Gurugram
122102, India

Complete contact information is available at:
<https://pubs.acs.org/10.1021/acs.inorgchem.0c00752>

Notes

The authors declare no competing financial interest.

ACKNOWLEDGMENTS

One of the authors, Sneha Yadav, thanks the Council of Scientific & Industrial Research (CSIR), New Delhi, India, for a Senior Research Fellowship and also acknowledges USIC-CLF, DU for characterizations including XRD, SEM, EDX, FTIR, VSM analyses, and TERI (Gurugram, India) for TEM analysis.

REFERENCES

- (1) Mueller, U.; Schubert, M.; Teich, F.; Puetter, H.; Schierle-Arndt, K.; Pastre, J. Metal–organic frameworks—prospective industrial applications. *J. Mater. Chem.* **2006**, *16*, 626–636.
- (2) Czaja, A. U.; Trukhan, N.; Müller, U. Industrial applications of metal–organic frameworks. *Chem. Soc. Rev.* **2009**, *38*, 1284–1293.
- (3) Rogge, S. M. J.; Bavykina, A.; Hajek, J.; Garcia, H.; Olivoso-Suarez, A. I.; Sepulveda-Escribano, A.; Vimont, A.; Clet, G.; Bazin, P.; Kapteijn, F.; Daturi, M.; Ramos-Fernandez, E. V.; Llabres i Xamena, F. X.; Van Speybroeck, V.; Gascon, J. Metal–organic and covalent organic frameworks as single-site catalysts. *Chem. Soc. Rev.* **2017**, *46*, 3134–3184.
- (4) Horcajada, P.; Gref, R.; Baati, T.; Allan, P. K.; Maurin, G.; Couvreur, P.; Ferey, G.; Morris, R. E.; Serre, C. Metal–organic frameworks in biomedicine. *Chem. Rev.* **2012**, *112*, 1232–1268.
- (5) Silva, P.; Vilela, S. M. F.; Tome, J. P. C.; Almeida Paz, F. A. Multifunctional metal–organic frameworks: from academia to industrial applications. *Chem. Soc. Rev.* **2015**, *44*, 6774–6803.
- (6) Mazaj, M.; Birsa Čelič, T.; Mali, G.; Rangus, M.; Kaučič, V.; Zabukovec Logar, N. Control of the crystallization process and structure dimensionality of Mg–Benzene–1, 3, 5-tricarboxylates by tuning solvent composition. *Cryst. Growth Des.* **2013**, *13*, 3825–3834.
- (7) Zacher, D.; Schmid, R.; Woell, C.; Fischer, R. A. Surface chemistry of metal–organic frameworks at the liquid–solid interface. *Angew. Chem., Int. Ed.* **2011**, *50*, 176–199.
- (8) Haldar, R.; Maji, T. K. Metal–organic frameworks (MOFs) based on mixed linker systems: structural diversities towards functional materials. *CrystEngComm* **2013**, *15*, 9276–9295.
- (9) Zhu, Q. L.; Xu, Q. Metal–organic framework composites. *Chem. Soc. Rev.* **2014**, *43*, 5468–5512.
- (10) Zhou, H. C.; Long, J. R.; Yaghi, O. M. Introduction to metal–organic frameworks. *Chem. Rev.* **2012**, *112*, 673–674.
- (11) Liu, J.; Chen, L.; Cui, H.; Zhang, J.; Zhang, L.; Su, C. Y. Applications of metal–organic frameworks in heterogeneous supra-molecular catalysis. *Chem. Soc. Rev.* **2014**, *43*, 6011–6061.
- (12) Wang, J. S.; Jin, F. Z.; Ma, H. C.; Li, X. B.; Liu, M. Y.; Kan, J. L.; Chen, G. J.; Dong, Y. B. Au@Cu(II)-MOF: Highly efficient bifunctional heterogeneous catalyst for successive oxidation–condensation reactions. *Inorg. Chem.* **2016**, *55*, 6685–6691.
- (13) Dhakshinamoorthy, A.; Alvaro, M.; Garcia, H. Commercial metal–organic frameworks as heterogeneous catalysts. *Chem. Commun.* **2012**, *48*, 11275–11288.
- (14) Chughtai, A. H.; Ahmad, N.; Younus, H. A.; Laypkov, A.; Verpoort, F. Metal–organic frameworks: versatile heterogeneous catalysts for efficient catalytic organic transformations. *Chem. Soc. Rev.* **2015**, *44*, 6804–6849.
- (15) Ye, R. P.; Lin, L.; Chen, C. C.; Yang, J. X.; Li, F.; Zhang, X.; Li, D. J.; Qin, Y. Y.; Zhou, Z.; Yao, Y. G. Synthesis of Robust MOF-Derived Cu/SiO₂ Catalyst with Low Copper Loading via Sol–Gel Method for the Dimethyl Oxalate Hydrogenation Reaction. *ACS Catal.* **2018**, *8*, 3382–3394.
- (16) Qu, B. T.; Lai, J. C.; Liu, S.; Gao, Y. D.; You, X. Z. Cu- and Ag-Based Metal–Organic Frameworks with 4-Pyranone-2, 6-dicarboxylic Acid: Syntheses, Crystal Structures, and Dielectric Properties. *Cryst. Growth Des.* **2015**, *15*, 1707–1713.
- (17) Hinde, C. S.; Webb, W. R.; Chew, B. K.; Tan, H. R.; Zhang, W. H.; Hor, T. A.; Raja, R. Utilisation of gold nanoparticles on amine-functionalised UiO-66 (NH₂-UiO-66) nanocrystals for selective tandem catalytic reactions. *Chem. Commun.* **2016**, *52*, 6557–6560.
- (18) Yuan, J.; Fracaro, A. M.; Klemperer, W. G. Convergent Synthesis of a Metal–Organic Framework Supported Olefin Metathesis Catalyst. *Organometallics* **2016**, *35*, 2149–2155.
- (19) Genna, D. T.; Wong-Foy, A. G.; Matzger, A. J.; Sanford, M. S. Heterogenization of homogeneous catalysts in metal–organic frameworks via cation exchange. *J. Am. Chem. Soc.* **2013**, *135*, 10586–10589.
- (20) Breeze, M. I.; Clet, G.; Campo, B. C.; Vimont, A.; Daturi, M.; Greneche, J.-M.; Dent, A. J.; Millange, F.; Walton, R. I. Isomorphous Substitution in a Flexible Metal–Organic Framework: Mixed-Metal, Mixed-Valent MIL-53 Type Materials. *Inorg. Chem.* **2013**, *52*, 8171–8182.
- (21) Liu, Y. Y.; Leus, K.; Bogaerts, T.; Hemelsoet, K.; Bruneel, E.; Van Speybroeck, V.; Van Der Voort, P. Bimetallic–Organic Framework as a Zero-Leaching Catalyst in the Aerobic Oxidation of Cyclohexene. *ChemCatChem* **2013**, *5*, 3657–3664.
- (22) Wu, P.; Guo, X.; Cheng, L.; He, C.; Wang, J.; Duan, C. Photoactive Metal–Organic Framework and Its Film for Light-Driven Hydrogen Production and Carbon Dioxide Reduction. *Inorg. Chem.* **2016**, *55*, 8153–8159.
- (23) Thompson, A. B.; Pahls, D. R.; Bernales, V.; Gallington, L. C.; Malonzo, C. D.; Webber, T.; Tereniak, S. J.; Wang, T. C.; Desai, S. P.; Li, Z.; Kim, I. S.; Gagliardi, L.; Penn, R. L.; Chapman, K. W.; Stein, A.; Farha, O. K.; Hupp, J. T.; Martinson, A. B. F.; Lu, C. C. Installing heterobimetallic cobalt–aluminum single sites on a metal organic framework support. *Chem. Mater.* **2016**, *28*, 6753–6762.
- (24) Cai, G.; Ding, M.; Wu, Q.; Jiang, H. L. Encapsulating soluble active species into hollow crystalline porous capsules beyond integration of homogeneous and heterogeneous catalysis. *Natl. Sci. Rev.* **2020**, *7*, 37–45.
- (25) Wang, S. S.; Jiao, L.; Qian, Y.; Hu, W. C.; Xu, G. Y.; Wang, C.; Jiang, H. L. Boosting Electrocatalytic Hydrogen Evolution over Metal–Organic Frameworks by Plasmon-Induced Hot-Electron Injection. *Angew. Chem., Int. Ed.* **2019**, *58*, 10713–10717.
- (26) Yang, Q.; Xu, Q.; Jiang, H. L. Metal–organic frameworks meet metal nanoparticles: synergistic effect for enhanced catalysis. *Chem. Soc. Rev.* **2017**, *46*, 4774–4808.
- (27) Ricco, R.; Malfatti, L.; Takahashi, M.; Hill, A. J.; Falcaro, P. Applications of magnetic metal–organic framework composites. *J. Mater. Chem. A* **2013**, *1*, 13033–13045.
- (28) Zhao, X.; Liu, S.; Tang, Z.; Niu, H.; Cai, Y.; Meng, W.; Wu, F.; Giesy, J. P. Synthesis of magnetic metal–organic framework (MOF) for efficient removal of organic dyes from water. *Sci. Rep.* **2015**, *5*, 11849.
- (29) Chen, Y.; Xiong, Z.; Peng, L.; Gan, Y.; Zhao, Y.; Shen, J.; Qian, J.; Zhang, L.; Zhang, W. Facile preparation of core–shell magnetic metal–organic framework nanoparticles for the selective capture of phosphopeptides. *ACS Appl. Mater. Interfaces* **2015**, *7*, 16338–16347.
- (30) Li, Y.; Xie, Q.; Hu, Q.; Li, C.; Huang, Z.; Yang, X.; Guo, H. Surface modification of hollow magnetic Fe₃O₄@NH₂-MIL-101(Fe) derived from metal–organic frameworks for enhanced selective removal of phosphates from aqueous solution. *Sci. Rep.* **2016**, *6*, 30651.
- (31) Huang, L.; Cai, J.; He, M.; Chen, B.; Hu, B. Room-Temperature Synthesis of Magnetic Metal–Organic Frameworks Composites in Water for Efficient Removal of Methylene Blue and As (V). *Ind. Eng. Chem. Res.* **2018**, *57*, 6201–6209.

- (32) Kolb, H. C.; Finn, M. G.; Sharpless, K. B. Click chemistry: diverse chemical function from a few good reactions. *Angew. Chem., Int. Ed.* **2001**, *40*, 2004–2021.
- (33) Marrocchi, A.; Facchetti, A.; Lanari, D.; Santoro, S.; Vaccaro, L. Click-chemistry approaches to π -conjugated polymers for organic electronics applications. *Chem. Sci.* **2016**, *7*, 6298–6308.
- (34) Deraedt, C.; Pinaud, N.; Astruc, D. Recyclable catalytic dendrimer nanoreactor for part-per-million CuI catalysis of “click” chemistry in water. *J. Am. Chem. Soc.* **2014**, *136*, 12092–12098.
- (35) Agalave, S. G.; Maujan, S. R.; Pore, V. S. Click chemistry: 1, 2, 3-triazoles as pharmacophores. *Chem. - Asian J.* **2011**, *6*, 2696–2718.
- (36) Bai, Y.; Feng, X.; Xing, H.; Xu, Y.; Kim, B. K.; Baig, N.; Zhou, T.; Gewirth, A. A.; Lu, Y.; Oldfield, E.; Zimmerman, S. C. A highly efficient single-chain metal–organic nanoparticle catalyst for alkyne–azide “click” reactions in water and in cells. *J. Am. Chem. Soc.* **2016**, *138*, 11077–11080.
- (37) Shin, J. A.; Lim, Y. G.; Lee, K. H. Copper-catalyzed azide–alkyne cycloaddition reaction in water using cyclodextrin as a phase transfer catalyst. *J. Org. Chem.* **2012**, *77*, 4117–4122.
- (38) Nakamura, T.; Terashima, T.; Ogata, K.; Fukuzawa, S. I. Copper (I) 1, 2, 3-triazol-5-ylidene complexes as efficient catalysts for click reactions of azides with alkynes. *Org. Lett.* **2011**, *13*, 620–623.
- (39) Liu, M.; Reiser, O. A copper (I) isonitrile complex as a heterogeneous catalyst for azide–alkyne cycloaddition in water. *Org. Lett.* **2011**, *13*, 1102–1105.
- (40) Jia, Q.; Yang, G.; Chen, L.; Du, Z.; Wei, J.; Zhong, Y.; Wang, J. A Facile One-Pot Metal-Free Synthesis of 1, 4-Disubstituted 1, 2, 3-Triazoles. *Eur. J. Org. Chem.* **2015**, *2015*, 3435–3440.
- (41) Xiong, X.; Cai, L. Application of magnetic nanoparticle-supported CuBr: A highly efficient and reusable catalyst for the one-pot and scale-up synthesis of 1, 2, 3-triazoles under microwave-assisted conditions. *Catal. Sci. Technol.* **2013**, *3*, 1301–1307.
- (42) Jahanshahi, R.; Akhlaghinia, B. Cu II immobilized on guanidinated epibromohydrin functionalized γ -Fe₂O₃@TiO₂(γ -Fe₂O₃@TiO₂-EG-CuII): a novel magnetically recyclable heterogeneous nanocatalyst for the green one-pot synthesis of 1, 4-disubstituted 1, 2, 3-triazoles through alkyne–azide cycloaddition in water. *RSC Adv.* **2016**, *6*, 29210–29219.
- (43) Anil Kumar, B.S.P.; Harsha Vardhan Reddy, K.; Madhav, B.; Ramesh, K.; Nageswar, Y.V.D. Magnetically separable CuFe₂O₄ nanoparticles catalyzed multicomponent synthesis of 1, 4-disubstituted 1, 2, 3-triazoles in tap water using ‘click chemistry’. *Tetrahedron Lett.* **2012**, *53*, 4595–4599.
- (44) Tavassoli, M.; Landarani-Isfahani, A.; Moghadam, M.; Tangestaninejad, S.; Mirkhani, V.; Mohammadpoor-Baltork, I. Copper dithiol complex supported on silica nanoparticles: A sustainable, efficient, and eco-friendly catalyst for multicomponent click reaction. *ACS Sustainable Chem. Eng.* **2016**, *4*, 1454–1462.
- (45) Veerakumar, P.; Velayudham, M.; Lu, K. L.; Rajagopal, S. Highly dispersed silica-supported nanocopper as an efficient heterogeneous catalyst: application in the synthesis of 1, 2, 3-triazoles and thioethers. *Catal. Sci. Technol.* **2011**, *1*, 1512–1525.
- (46) Nasr-Esfahani, M.; Mohammadpoor-Baltork, I.; Khosropour, A. R.; Moghadam, M.; Mirkhani, V.; Tangestaninejad, S.; Amiri Rudbari, H. Copper Immobilized on Nanosilica Triazine Dendrimer (Cu (II)-TD@nSiO₂)-Catalyzed Regioselective synthesis of 1, 4-disubstituted 1, 2, 3-triazoles and bis-and tris-Triazoles via a one-pot multicomponent click reaction. *J. Org. Chem.* **2014**, *79*, 1437–1443.
- (47) Gholinejad, M.; Jeddi, N. Copper nanoparticles supported on agarose as a bioorganic and degradable polymer for multicomponent click synthesis of 1, 2, 3-triazoles under low copper loading in water. *ACS Sustainable Chem. Eng.* **2014**, *2*, 2658–2665.
- (48) Sabaqian, S.; Nemati, F.; Heravi, M. M.; Nahzomi, H. T. Copper (I) iodide supported on modified cellulose-based nanomagnetite composite as a biodegradable catalyst for the synthesis of 1, 2, 3-triazoles. *Appl. Organomet. Chem.* **2017**, *31*, e3660.
- (49) Alonso, F.; Moglie, Y.; Radivoy, G.; Yus, M. Multicomponent Synthesis of 1, 2, 3-Triazoles in Water Catalyzed by Copper Nanoparticles on Activated Carbon. *Adv. Synth. Catal.* **2010**, *352*, 3208–3214.
- (50) Salamatmanesh, A.; Kazemi Miraki, M.; Yazdani, E.; Heydari, A. Copper (I)–Caffeine Complex Immobilized on Silica-Coated Magnetite Nanoparticles: A Recyclable and Eco-friendly Catalyst for Click Chemistry from Organic Halides and Epoxides. *Catal. Lett.* **2018**, *148*, 3257–3268.
- (51) Sharma, P.; Rathod, J.; Singh, A. P.; Kumar, P.; Sasson, Y. Synthesis of heterogeneous Ru (ii)-1, 2, 3-triazole catalyst supported over SBA-15: application to the hydrogen transfer reaction and unusual highly selective 1, 4-disubstituted triazole formation via multicomponent click reaction. *Catal. Sci. Technol.* **2018**, *8*, 3246–3259.
- (52) Kazemi Movahed, S.; Salari, P.; Kasmaei, M.; Armaghan, M.; Dabiri, M.; Amini, M. M. Copper nanoparticles incorporated on a mesoporous carbon nitride, an excellent catalyst in the Huisgen 1, 3-dipolar cycloaddition and N-arylation of N-heterocycles. *Appl. Organomet. Chem.* **2018**, *32*, e3914.
- (53) Gupta, R.; Yadav, M.; Gaur, R.; Arora, G.; Sharma, R. K. A straightforward one-pot synthesis of bioactive N-aryl oxazolidin-2-ones via a highly efficient Fe₃O₄@SiO₂-supported acetate-based butylimidazolium ionic liquid nanocatalyst under metal-and solvent-free conditions. *Green Chem.* **2017**, *19*, 3801–3812.
- (54) Sharma, R. K.; Gaur, R.; Yadav, M.; Goswami, A.; Zboril, R.; Gawande, M. B. An efficient copper-based magnetic nanocatalyst for the fixation of carbon dioxide at atmospheric pressure. *Sci. Rep.* **2018**, *8*, 1901.
- (55) Rana, P.; Gaur, R.; Gupta, R.; Arora, G.; Jayashree, A.; Sharma, R. K. Cross-dehydrogenative C(sp³)-C(sp³) coupling via CH activation using magnetically retrievable ruthenium-based photoredox nanocatalyst under aerobic conditions. *Chem. Commun.* **2019**, *55*, 7402–7405.
- (56) Sharma, R. K.; Gaur, R.; Yadav, M.; Rath, A. K.; Pechousek, J.; Petr, M.; Zboril, R.; Gawande, M. B. Maghemite-Copper Nanocomposites: Applications for Ligand-Free Cross-Coupling (C–O, C–S, and C–N) Reactions. *ChemCatChem* **2015**, *7*, 3495–3502.
- (57) Sharma, R. K.; Dutta, S.; Sharma, S. Quinoline-2-carboimine copper complex immobilized on amine functionalized silica coated magnetite nanoparticles: a novel and magnetically retrievable catalyst for the synthesis of carbamates via C–H activation of formamides. *Dalton Trans.* **2015**, *44*, 1303–1316.
- (58) Sharma, R. K.; Yadav, M.; Monga, Y.; Gaur, R.; Adholeya, A.; Zboril, R.; Varma, R. S.; Gawande, M. B. Silica-based Magnetic Manganese Nanocatalyst–Applications in the Oxidation of Organic Halides and Alcohols. *ACS Sustainable Chem. Eng.* **2016**, *4*, 1123–1130.
- (59) Sharma, R. K.; Monga, Y.; Puri, A.; Gaba, G. Magnetite (Fe₃O₄) silica based organic–inorganic hybrid copper (ii) nanocatalyst: a platform for aerobic N-alkylation of amines. *Green Chem.* **2013**, *15*, 2800–2809.
- (60) Yang, J.-C.; Yin, X.-B. CoFe₂O₄@MIL-100 (Fe) hybrid magnetic nanoparticles exhibit fast and selective adsorption of arsenic with high adsorption capacity. *Sci. Rep.* **2017**, *7*, 40955.
- (61) Hu, H.; Lou, X.; Li, C.; Hu, X.; Li, T.; Chen, Q.; Shen, M.; Hu, B. A thermally activated manganese 1, 4-benzenedicarboxylate metal organic framework with high anodic capability for Li-ion batteries. *New J. Chem.* **2016**, *40*, 9746–9752.
- (62) Ren, C.; Ding, X.; Fu, H.; Li, W.; Wu, H.; Yang, H. Core–shell superparamagnetic monodisperse nanospheres based on amino-functionalized CoFe₂O₄@SiO₂ for removal of heavy metals from aqueous solutions. *RSC Adv.* **2017**, *7*, 6911–6921.
- (63) Fu, Y. L.; Ren, J. L.; Qiao, H. P.; Ng, S. W. The 1:2/3 adduct of manganese (II) terephthalate with N, N-dimethylformamide. *Acta Crystallogr., Sect. E: Struct. Rep. Online* **2004**, *60*, m1510–m1512.